



The Potency of *Adenostemma platyphyllum* as Antimelanogenic Agent: *In-vitro* and *In-silico* Studies

Lutfia Mutmainnah¹, Irmanida Batubara^{1,2,*}, Auliya Ilmiawati^{1,2}

¹ Department of Chemistry, Faculty of Mathematics and Natural Sciences, IPB University, Bogor, Indonesia

² Tropical Biopharmaca Research Center, IPB University, Bogor, Indonesia

* Corresponding author: ime@apps.ipb.ac.id

<https://doi.org/10.14710/jksa.27.5.232-242>



Article Info

Article history:

Received: 02nd February 2024

Revised: 16th May 2024

Accepted: 21st May 2024

Online: 31st May 2024

Keywords:

Asteraceae; docking; skin whitening; tyrosinase inhibition

Abstract

Melanin is a crucial amino acid in determining human skin and hair pigmentation. Excessive melanin production can lead to hyperpigmentation and darkening of the skin. This study aims to assess the capability of *Adenostemma platyphyllum* as a tyrosinase enzyme inhibitor. It predicts its anti-melanogenic activity through molecular docking with proteins involved in the melanogenesis process. The *in-vitro* approach was conducted by determining the tyrosinase enzyme inhibition capacity, while the *in-silico* approach involved ligand binding to target proteins from melanogenesis pathways. The highest tyrosinase inhibition capacity was observed in the ethanol extract, with values of 9.74 Kojic Acid Equivalent (KAE)/g extract (*L*-tyrosine) and 17.91 (KAE)/g extract (*L*-DOPA). Molecular docking analysis showed that the binding of eriodictyol 7-*O*-sophoroside ($\Delta G = -9.7$ kcal/mol) has the best energy affinity for the PKC- β protein, genistein ($\Delta G = -7.5$ kcal/mol) for the tyrosinase-related protein-1 (TYRP1) protein, eriodictyol 7-*O*-sophoroside ($\Delta G = -10.2$ kcal/mol) for the cGMP protein, vincosamide ($\Delta G = -7.2$ kcal/mol) for the microphthalmia-associated transcription factor (MITF) protein, and dicaffeoylquinic acid ($\Delta G = -7.4$ kcal/mol) for the β -catenin protein. Based on a comparison of *in-vitro* and *in-silico* studies, melanogenesis inhibition is more potent in the PKC- β and cGMP pathways than direct tyrosinase inhibition because they exhibit lower binding energy.

1. Introduction

Skin issues such as dark spots, excessive skin darkening, and hyperpigmentation commonly occur on the skin, specifically on the face. These problems include skin inflammation, excessive exposure to sunlight (UV), skin aging processes, use of certain medications, hemochromatosis, and overproduction of melanin. Melanin, a complex polymer produced from the amino acid tyrosine, plays a crucial role in determining the color of human skin and hair through a process known as melanogenesis. Skin-whitening agents with anti-melanogenic properties or the ability to inhibit melanogenesis are products used to reduce melanin production in the skin, addressing hyperpigmentation issues and brightening skin tone. Commercially, commonly used compounds as skin-whitening agents include hydroquinone, kojic acid, arbutin, and ascorbic

acid. Most of these compounds are synthetic, and prolonged excessive use can lead to side effects such as skin irritation, redness, burning sensation, and even skin cancer [1]. Therefore, there is a need for alternative compounds derived from plants to minimize these side effects.

Plants of the Asteraceae family, genus *Adenostemma*, are known to contain various secondary metabolites such as flavonoids, alkaloids, and terpenoids. One species, *Adenostemma lavenia*, has been reported to exhibit potent antioxidant and antiglycation activities and anti-melanogenic and anti-inflammatory activities [2, 3]. The leaf extract of *A. lavenia* contains kaurenoic acid (11 α OH-KA), responsible for 50% of its anti-melanogenic activity [4]. Another species within the same genus, *Adenostemma platyphyllum*, has been reported for its antitussive or cough medicine, analgesic, and traditional medicinal uses

such as acne treatment, snakebite, and scorpion sting remedy [5].

Additionally, Nurlela *et al.* [6] summarized the potential activities of *A. platyphyllum* from various sources, including antibacterial, anti-inflammatory, and antioxidant activities. This potential activity is attributed to the plant's total phenolic compounds (TPC) and total flavonoid compounds (TFC) measured at 5.01 mg GAE/g DW and 3.48 QE/g DW. Phenolic compounds such as eriodictyol [7] and caffeoylquinic acid [8] and diterpene compounds such as hydroxykaurenoic acid [4] are known to possess antimelanogenic activity against B16F10 cells. These compounds are present in *A. platyphyllum* [9]. This presence indicates the potential of *A. platyphyllum* for antimelanogenic activity.

This study aims to investigate the inhibition of the tyrosinase enzyme through *in-vitro* testing using two substrates, *L*-DOPA and *L*-Tyrosine. *In-silico* studies are conducted to complement *in-vitro* investigations as a comparative analysis of melanogenesis pathway inhibition. Three main pathways produce and regulate the melanin production process or melanogenesis: the cAMP pathway, PKC- β pathway, and NO pathway (Figure 1). Each path involves specific proteins, namely microphthalmia-associated transcription factor (MITF) and tyrosinase-related protein 1 in the cAMP pathway, protein kinase C- β in the PKC- β pathway, and cyclic GMP in the NO pathway.

Additionally, there is another alternative pathway through the wingless-related integration site (WNT) signaling with the β -catenin protein. The melanogenesis pathway will be inhibited through molecular docking with MITF protein (PDB ID 7EOD), tyrosinase-related protein 1 (PDB ID 5M8R), protein kinase C β (PDB ID 2I0E), cyclic GMP (PDB ID 6LRC), and β -catenin (PDB ID 7UWI). According to existing literature, there is no reported evidence of the potential of *A. platyphyllum* as an anti-melanogenic agent through *in-vitro* and *in-silico* methods. Therefore, the objective of this article is to assess the capability of *A. platyphyllum* as a tyrosinase enzyme inhibitor and predict its anti-melanogenic activity through molecular docking with proteins involved in the melanogenesis process.

2. Experimental

2.1. Plant Materials and Extraction Methods

A. platyphyllum leaves were collected from the Biopharmaca Conservation and Cultivation Station, Tropical Biopharmaca Research Center, IPB University, located at 6°32'25.47" N and 106°42'53.22" E, at 142.60 m altitude. The sample was dried and sifted to leaf powder. About 600 g of leaf powder was extracted by increasing the polarity of solvents (600 mL). First, *n*-hexane was used as a solvent. Extraction was continued to the residue using ethyl acetate and ethanol. With different *A. platyphyllum* leaf, powder was extracted in hot water (55°C). The yield of all extracts was determined after the extract was dried.

2.2. Phytochemicals Test

2.2.1. Alkaloid

Referring to Pant *et al.* [10], the diluted extract was placed in a suitable solvent and added to a reaction tube. The reaction tube, filled with the filtrate, was mixed with 1 mL of 2 M H₂SO₄ until two separate layers formed. The two layers were then separated. Meyer, Wagner, and Dragendorff reagents were added drop by drop to the acidic layer.

2.2.2. Triterpenoid and Steroid

A 0.05 g of the extract was diluted with 5 mL of hot ethanol and filtered into a reaction tube. The filtrate was evaporated to dryness, and 1 mL of diethyl ether was added before transferring it to an evaporation dish. Concentrated H₂SO₄ and one drop of anhydrous CH₃COOH were added to the solution.

2.2.3. Flavonoid

A 0.05 g of the extract was diluted with 5 mL of distilled water and boiled for 5 minutes before filtering. The resulting filtrate was added to magnesium powder, 1 mL of HCl, 1 mL of ethanol, and 1 mL of amyl alcohol. The mixture was then vigorously shaken for several minutes.

2.2.4. Saponin

A 0.05 g of the extract was diluted with 5 mL of distilled water and boiled for 5 minutes before filtering. The resulting filtrate was vigorously shaken until foam formed.

2.2.5. Tannin

A 0.05 g of the extract was diluted with 5 mL of distilled water and boiled for 5 minutes before filtering. Several drops of 10% FeCl₃ were added to the filtrate. In phytochemical tests, a positive control was used as a reference to compare the intensity of the tested extract with the control. The plant used as the control had been reported to contain the tested compounds positively.

2.3. Tyrosinase Inhibition Assay

Tyrosinase inhibition assay followed the methods of Batubara *et al.* [11] and Budiarti *et al.* [12]. An initial solution was prepared at a concentration of 10,000 mg mL⁻¹, and subsequent dilutions were made with 50 mM phosphate buffer (pH 6.5). A 70 μ L of the extract was added to each well in a microplate, followed by the addition of 30 μ L of tyrosinase enzyme (Carbosynth, 333 Units mL⁻¹ in phosphate buffer). The microplate was then incubated at 37°C for 5 minutes. Subsequently, the substrate (2 μ M *L*-tyrosine or 2 μ M *L*-DOPA) was added to each well, and the plate was further incubated for 30 minutes. Absorbance values were determined using a multi-well reader at a wavelength of 492 nm. Kojic acid was used as a standard with concentrations of 1–62.5 μ g mL⁻¹ for *L*-DOPA substrate and 1–31.25 μ g mL⁻¹ for *L*-tyrosine substrate. The tyrosinase enzyme inhibition capacity was reported in kojic acid equivalents (KAE)/g of extract.

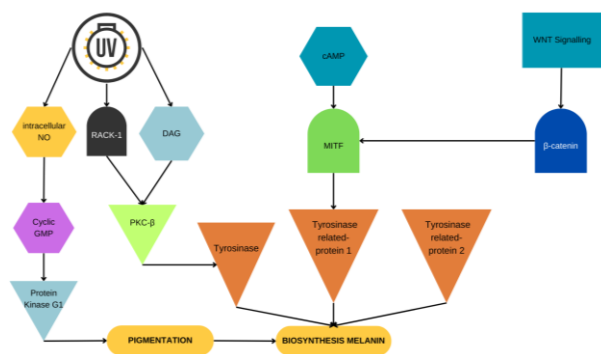


Figure 1. Melanogenesis pathways

2.4. Molecular Docking

Protein structures were sourced from the RCSB Protein Data Bank (<https://www.rcsb.org/>). The chosen protein structures included MITF (PDB ID 7EOD), TYRP1 (PDB ID 5M8R), PKCβ (PDB ID 2IoE), cyclic GAMP (PDB ID 6LRC), and β-catenin (PDB ID 7UWI) represent each melanogenesis pathway (as depicted in Figure 1). The proteins were selected based on specific criteria: resolution 1.8–2.6 Å, origin from Homo sapiens organisms, and acquisition through X-ray diffraction data. Undesirable components such as protein chains, water molecules, metal atoms, and co-crystallized ligands were removed using PyMOL [13]. PyMOL, Available at: <http://www.pymol.org/pymol>. Missing residues were fixed using the SWISS-MODEL site (<https://swissmodel.expasy.org>) [14]. Polar hydrogen atoms were added, and a grid box was established with AutoDockTools [15] to position the ligand-binding site based on the lowest energy found during scanning.

The resulting configurations were saved in PDBQT format. The 3D structures of ligands from 25 compounds of *A. platyphyllum* [9] were retrieved from PubChem (<https://pubchem.ncbi.nlm.nih.gov/>) [16]. Ligand structures were converted to PDB format using OpenBabel [17], optimized with AutoDockTools, and saved in PDBQT format. AutoDock Vina [18, 19] was used for molecular docking. It was validated by redocking co-crystallized ligands removed from their respective

proteins and blind docking with control ligand coordinates. Docked molecules binding energy values (ΔG , kcal/mol) constituted the data and LigPlot+ [20] analyzed ligand-protein binding features for ligands with the lowest energy in each protein.

2.5. Pharmacokinetics, Toxicity, and Bioactivity

The structure of the selected test ligands was converted to *.SMILES format using the OpenBabel program. This conversion was carried out because the pharmacokinetic analysis prediction page only accepts line notation for encoding a molecular structure. After conversion, the test ligand was critically evaluated for its adherence to Lipinski’s rules, a crucial step in drug development. It was then predicted based on absorption, distribution, metabolism, excretion, and toxicity (ADMET) parameters (on the page <https://biosig.lab.uq.edu.au/pkcsdm/prediction>) as well as PASS prediction or bioactivity ligands on the page <https://www.way2drug.com/passonline/>.

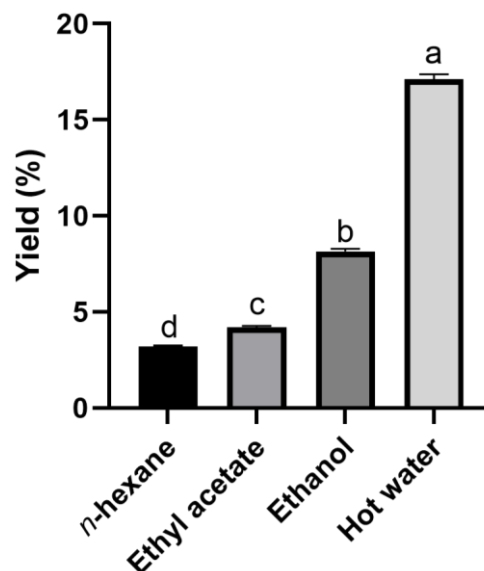


Figure 2. Yield of *A. platyphyllum* extract in various solvents. Different letters indicate significantly different values at the 95% confidence interval

Table 1. Phytochemicals of *A. platyphyllum* extract in various solvents

Solvent	<i>n</i> -hexane	Ethyl acetate	Ethanol	Hot water	Positive control	Reference of positive control
Alkaloid	-	-	-	-	++++ (Madagascar periwinkle flower)	[21]
Flavonoid	++	++	+	-	++++ (Piper ornatum leaf)	[22]
Saponin	-	-	-	+++	++++ (Sapindus rarak fruit)	[23]
Tanin	-	-	-	+	++++ (Camellia sinensis powder)	[24]
Steroid	+	+++	+++	-	++++ (Ocimum leaf ethanol extract)	[25]
Triterpenoid	-	-	-	-	++++ (Ocimum leaf)	[26]

Note: The positive parameters relative to the positive control. (++++) highly positive, (+++) positive, (++) moderately positive, (+) mildly positive, (-) none

Table 2. Tyrosinase inhibition capacity

Extract	Capacity (mg KAE/g extract)	
	L-tyrosine	L-DOPA
<i>n</i> -hexane	-	8.50±0.58 ^d
Ethyl acetate	-	13.62±0.67 ^b
Ethanol	9.74±0.04 ^c	17.91±0.08 ^a
Hot water	4.28±0.03 ^e	17.83±0.29 ^a

Note: Different letters indicate significantly different values at the 95% confidence interval; (-): not detected

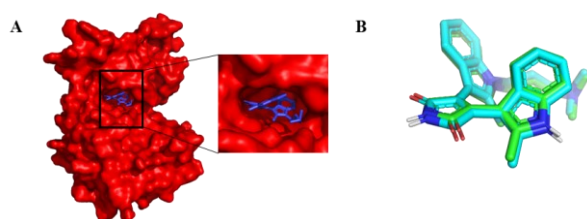


Figure 3. Docking results of one of the (A) protein structures (2IOE) and (B) comparison of cocrystal ligands before and after redocking

3. Results and Discussion

3.1. Yield and Moisture Content of *Adenostemma platyphyllum*

The extraction of *A. platyphyllum* yielded results, as shown in Figure 2. In the *A. platyphyllum* plant, the highest to lowest yields were obtained in the following order: hot water extract, ethanol, ethyl acetate, and *n*-hexane (17.12±0.26%, 8.16±0.13%, 4.19±0.08%, and 3.21±0.04%). It can be speculated that polar and semi-polar compounds are more abundant in *A. platyphyllum* than nonpolar compounds. This is supported by the studies of Fauzan *et al.* [27] and Nurlela *et al.* [9], which reported that the main compounds in *A. platyphyllum* extract are aromatic compounds (phenolics), with phenolic compounds predominantly being polar and semi-polar.

The moisture content of *A. platyphyllum* was analyzed according to the standard method recommended by the Association of Official Analytical Chemists (AOAC) [28]. The moisture content of *A. platyphyllum* obtained was 11.45%. This result is higher than the findings of previous studies, such as Ananda [29], which received a yield of 8–9%, and Fauzan *et al.* [27] with a yield of 7%. Several factors may contribute to this difference, including air humidity, mineral supply, biotic effects, and salinity [30].

3.2. Phytochemicals Screening of *A. platyphyllum*

Qualitative phytochemical analysis is an initial screening tool to determine the presence of specific phytochemicals in plant samples. The results of the phytochemical screening of *A. platyphyllum* are presented in Table 1. The qualitative phytochemical screening of *A. platyphyllum* revealed that flavonoids, saponin, tannin, and steroids were present in the selected solvent; meanwhile, alkaloids and triterpenoids were not present in *A. platyphyllum*. Ethanol, *n*-hexane, and ethyl acetate exhibited flavonoids and steroids, while saponin and tannin only showed positive results in hot water extract.

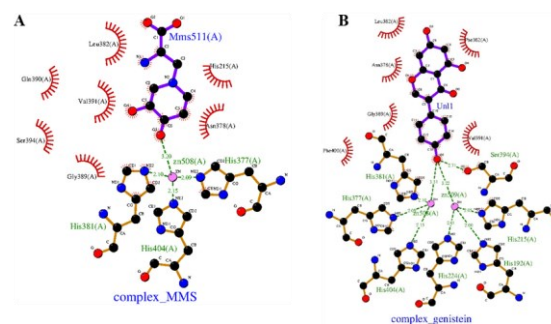


Figure 4. Interaction of tyrosinase 1 protein with (A) MMS and (B) genistein

Regarding yield data, hot water extract has the highest yield, but only saponins and tannins were detected in phytochemical screening. Consequently, the undetected compound groups in the hot water extract may likely consist of sugars and peptides. Nurlela *et al.* [9] reported that methanol extract from *A. platyphyllum* has several classes of major compounds, such as phenolic (phenolic acids, flavonols, flavones, isoflavones), alkaloids, diterpenes, and fatty acids. Differences in the polarity of the solvent can cause the differences in these compounds.

3.3. Tyrosinase Inhibition

The tyrosinase inhibition capacities of the four extracts can be seen in Table 2. The determination of tyrosinase inhibition capacity was calculated using the standard curve of kojic acid, with the results expressed in mg of kojic acid equivalents per gram of extract. The ethanol extract exhibited the highest inhibition capacity on the L-tyrosine substrate compared to the other three extracts. The *n*-hexane and ethyl acetate extracts on the L-tyrosine substrate showed no inhibition. The ethanol extract also demonstrated a higher capacity on the L-DOPA substrate than the other three extracts.

The tyrosinase inhibition capacity of the ethanol extract showed the highest results on both substrates, likely due to the presence of numerous semi-polar compounds in ethanol that actively act as tyrosinase inhibitors. Based on the review by Zolghadri *et al.* [31], active semi-polar compounds inhibiting tyrosinase include chalcones, flavonols, isoflavones, and carvacrol. Factors influencing this enzymatic reaction include substrate concentration, enzyme concentration, temperature, pH, the presence of cofactors/coenzymes, and inhibitors. These factors interact and can have complex effects on enzymatic reactions. Optimizing these factors is crucial to obtaining maximum results.

Table 3. Binding energy and RMSD values from redocking and blind docking of cocrystal and control ligands

Complex protein-ligand	Binding energy (kcal/mol)	RMSD (Å)
2I0E - PDS	-12.4	0.418
5M8R - MMS	-5.8	0.705
6LRC - KHM	-9.7	0.307
7EOD - CH5552074	-6.4	N/A
7UWI - Curcumin	-7.4	N/A

Note: N/A: (not available)

Fundamentally, tyrosinase inhibition refers to the process of blocking or suppressing the activity of the enzyme tyrosinase. Tyrosinase is a key enzyme involved in the biosynthesis of melanin, catalyzing the ortho-hydroxylation of tyrosine into 3,4-dihydroxyphenylalanine or DOPA (monophenolase) and the oxidation of DOPA into dopaquinone (diphenolase) [2]. The reaction process that occurs with the tyrosinase enzyme using *L*-tyrosine and *L*-DOPA as substrates can be observed by a change in color to dark brown, indicating the formation of a dopachrome [32].

3.4. Validation Molecular Docking

Molecular docking validation must be performed to compare and analyze differences in ligand locations before and after docking. The validation method is carried out in two ways: redocking (redocking of the cocrystal ligand) and blind docking (docking of the control ligand in the entire protein structure). The proteins validated by redocking were proteins 2I0E, 5M8R, and 6LRC, while proteins 7EOD and 7UWI were by blind docking.

The ligand is placed back into the protein's active site when redocking is performed. Ligand poses before and after docking are compared to understand the molecular interactions involved and evaluate the agreement between the two using RMSD values. The redocking method is valid if the RMSD value is ≤ 2.0 Å. Meanwhile, the blind docking method involves a control ligand looking for possible protein active sites, which are evaluated by the binding energy value of the control ligand. Three previously separated cocrystal ligands from the protein are tethered back to the original protein.

Figure 3 shows the redocking results of the 2I0E protein structure (colored red) with its cocrystal ligand, PDS (colored blue). After the redocking process, the cocrystal ligand poses before (colored green) and after redocking (colored light blue) were compared, and the RMSD values were obtained. In addition, protein-ligand binding energy data in kcal/mol were also obtained, which is recorded in Table 3. Two control ligands have been shown to inhibit target proteins, namely CH5552074 as an MITF inhibitor [33] and curcumin as a β -catenin inhibitor [34]. The ligand is tethered to the target protein, and the ligand with the highest binding energy is assumed

to be the protein's active site. Protein-ligand binding energy data in kcal/mol are recorded in Table 3.

3.5. Molecular Docking Analysis

The outcomes of molecular docking are presented as binding energies or docking scores (kcal/mol), where lower (more negative) values indicate a stronger binding affinity between the compound and the target protein. Table 4 lists the top three ligands with the highest binding affinities for each receptor protein. Subsequently, the ligands that exhibited the lowest energy for each protein were scrutinized for their protein-ligand interactions.

Table 4 also shows the amino acid residue interacting with the protein. If the test ligand has amino acid similarities with the cocrystal or control ligand of up to 50%, then the amino acid residue is amino acids, which plays a role in the protein's active site. These five proteins and their test ligands have >50% amino acid residue similarity. One example of visualization of protein-ligand interactions is shown in Figure 4. Arwansyah *et al.* [35] said that the potential for a test compound to inhibit the activity of a disease-causing target protein could be inferred from the resemblance of its amino acid residues and binding characteristics. When the amino acid residues closely resemble those of native ligands, it suggests that the ligands could effectively inhibit the target protein's activity.

One example of ligand interaction visualization can be seen in Figure 4. The Protein Kinase C- β (PDB ID 2I0E), eriodictyol 7-O-sophoroside exhibits the highest binding energy among other ligands. This ligand also binds to the identical amino acid residues as the co-crystallized ligand (Bisindolylmaleimide/PDS). Additionally, Grodsky *et al.* [36] showed that Asp470, Glu421, and Val423 are the residues in the active site of PKC- β . In the case of the TYRP1 protein (PDB ID 5M8R), genistein shows more interaction similarity with its co-crystallized ligand (Mimosine/MMS) compared to 2 ligands with the same binding energy. Moreover, genistein also binds to the active site of TYRP1 where, according to Lai *et al.* [37] His377, His381, His192, and Thr391 are the residues in the active site of TYRP1.

Table 4. The binding energy and molecular interactions of the top three identified compounds with receptor proteins

Receptor/Protein	Ligand (PubChem ID)	Binding free energy (kcal/mol)	Interacting residue	
			Hydrogen bond	Hydrophobic interactions
PKC- β (PDB ID 2I0E)	Eriodictyol 7-O-sophoroside (11541786)	-9.7	Asp470, Asp484, Glu421, Thr404, Tyr422, Val423	Ala369, Ala483, Leu348, Lys371, Met420, Met473, Phe353
	Cafestol (108052)	-9.3	N/A	Ala369, Ala483, Asp484, Leu348, Met420, Phe353, Val356
	N-methylidioncophylline A (14844756)	-9.2	N/A	Ala483, Leu348, Met420, Met473, Phe353, Thr404, Val356, Val423
	Vincosamide (10163855)	-9.2	N/A	Ala369, Ala483, Asp484, Glu421, Leu348, Met420, Met473, Phe353, Tyr422, Val423
	Hydroxykaurenoic acid	-9.2	N/A	Ala369, Ala483, Asp470, Asp484, Leu348, Met420, Phe353, Thr404, Val356
TYRP1 (PDB ID 5M8R)	PDS ⁽¹⁾	-9.2	Val423	Ala369, Ala483, Asn471, Asp470, Asp484, Gly349, Leu348, Met420, Met473, Phe353, Tyr422, Val356
	Genistein (5280961)	-7.5	His381, His404, His377, Ser394, His215	Gly389, Leu382, Asn378, Val391
	Hydroxy kaurenoic acid	-7.5	Asn378	Leu382, Gly389, His381, Val391, His215, His377
	Cafestol (108052)	-7.5	Asn378	Leu382, Gly389, His381, Val391, His377
	MMS ⁽¹⁾	-5.8	His381, His404, His377	Leu382, Gln390, Ser394, Leu382, Val391, Gly389, Asn378, His215
cGMP (PDB ID 6LRC)	Eriodictyol 7-O-sophoroside (11541786)	-10.2	His281, Leu334, Lys206	Arg220, Asn326, Phe332, Tyr280
	Vincosamide (10163855)	-9.7	N/A	Arg220, Leu221, Leu334, Lys206, Ser222, Ser278, Tyr280
	Kaempferol-3-O-galactoside (5282149)	-9.6	N/A	Arg220, Asn326, Ile329, Leu221, Lys206, Ser222, Ser278, Tyr280
	KHM ⁽¹⁾	-9.7	Arg220	Ala91, Asn326, Leu221, Leu334, Lys206, Phe332, Ser278, Tyr280
β -katenin (PDB ID 7UWI)	Vincosamide (10163855)	-7.2	Gly228, Trp241	Asn235, Asp236, Ile231, Lys233, Pro232, Pro237, Ser234
	Dihydroxykaurenoic acid	-7.0	N/A	Gly228, Ile231, Lys233, Pro232, Ser234, Trp241
	Grandiflorenic acid (161387)	-6.9	N/A	Gly228, Ile231, Lys233, Pro232, Ser234, Trp241
	CH5552074 ⁽²⁾	-6.4	Ser234	Asn235, Asp236, Gly228, Ile231, Lys233, Met239, Pro232, Pro237, Trp241
	Dicaffeoylquinic acid (13604687)	-7.4	Thr339, Asp299, Asn290, Asn261	Ile296, His223, His260
β -katenin (PDB ID 7UWI)	Vincosamide (10163855)	-7.1	Ala295, Thr399	Ile296, His260, Trp338, Asp299, Lys335
	Eriodictyol 7-O-sophoroside (11541786)	-7.1	Asp299, His223, Asn261	Lys335, Ile296, Trp338
	Curcumin ⁽²⁾	-7.4	Thr339, Ala295, Asn261	Asp299, Trp338, His223, Ile296, His260, Lys335

Note: ⁽¹⁾co-crystallize ligand; ⁽²⁾controlled ligand; (N/A): not available

Table 5. ADMET, Lipinski's rule, and bioactivity of chosen ligand

Parameter	Ligand			
	Dicaffeoylquinic acid	Eriodictyol 7-O-sophoroside	Vincosamide	Genistein
ADMET				
Absorption				
Human intestinal absorption (%)	29.2	7.895	62.89	93.894
Skin permeability (log Kp)	-2.735	-2.735	-2.738	-2.735
Distribution				
BBB Permeability (log BB)	-2.001	-1.819	-1.267	-0.835
Metabolism				
CYP2C9 inhibitor	No	No	No	Yes
CYP2C19 inhibitor	No	No	No	Yes
CYP2D6 inhibitor	No	No	No	No
Excretion				
Total clearance	-0.068	0.168	0.414	0.232
Toxicity				
Acute Oral Toxicity	III	IV	III	II
Skin Sensitisation	No	No	No	No
Lipinski's Rule				
LogP	-0.35	-3.97	-0.43	2.58
Molecular Weight	516.45	612.53	498.53	270.24
Acceptor H	12	16	5	3
Donor H	7	10	5	1
Drug likeness	No	No	Yes	Yes
Bioactivity (Melanin Inhibitor)				
Pa	0.427	0.731		0.421
Pi	0.004	0.001	N/A	0.004

Note: (N/A): not available

The protein cyclic guanosine monophosphate (cGMP) (PDB ID: 6LRC) demonstrated a favorable binding affinity with eriodictyol 7-O-sophoroside ($\Delta G = -10.2$ kcal/mol), where this ligand exhibits a binding pattern similar to its co-crystallized ligand (PF-06928215/KHM) as well as Arg220, Phe332, Tyr280, and Lys206. The CH5552074 compound serves as a control ligand for the MITF protein (PDB ID 7EOD) due to its ability to decrease MITF production in melanoma cells [33]. The compound undergoes blind docking to generate coordinates with the lowest energy, which are then used as coordinates for the test ligand. MITF protein showed a favorable binding affinity with vincosamide with a binding score of -7.2 kcal/mol. The residues in the binding site were in accordance with those of the controlled ligand (CH5552074) to 7EOD, including Ser234, Asn235, Asp236, Gly228, Ile231, Lys233, Pro232, Pro237, and Trp241.

Employing the same method as for the MITF protein, the β -catenin protein (PDB ID 7UWI) utilizes the control ligand curcumin to determine docking coordinates. Curcumin is selected as the control ligand due to its ability

to inhibit cancer cell growth [34]. The β -catenin protein displayed a favorable binding affinity with N-methylionophylline A ($\Delta G = -7.4$ kcal/mol). This compound exhibited a strong binding affinity to 7UWI through hydrophobic interactions with Thr339, Asp299, Asn261, Ile296, His233, and His260.

In addition to binding energy, molecular docking also provides information about the residue interactions that occur. Two residue interactions exist in the protein-ligand complex, namely hydrogen bonds and hydrophobic interactions. Hydrogen bonds are crucial in determining the structure of proteins and how molecules interact at a molecular level. They provide stability to the protein's shape, preserving its intended form, while also adding precision to its interactions with other molecules [38]. Hydrophobic interactions are well known to be important in providing thermodynamic stability in the folded and unfolded states. Hydrophobic interactions are essential because proteins can biologically shrink their surface area and reduce unwanted interactions with water [39].

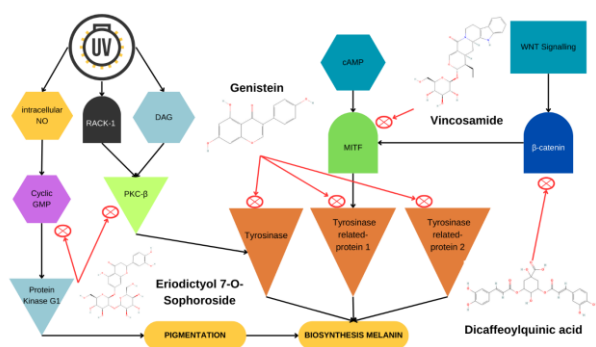


Figure 5. The potential anti-melanogenic mechanism for the active compound based on *in-silico* studies

3.6. Analysis of Pharmacokinetics, Toxicity, and Bioactivity of Chosen Ligand

Pharmacokinetics encompasses the investigation of the body's interactions with administered substances over the entire exposure period. Typically, this discipline focuses on four key aspects: absorption, distribution, metabolism, and excretion (ADME) [40]. Selected ligands from the five proteins, namely dicafeoylquinic acid, eriodictyol 7-O-sophoroside, vincosamide, and genistein, were each tested for their conformity with Lipinski's rules and predicted ADMET and bioactivity as shown in Table 5.

A ligand with less than 30% absorption in human intestinal absorption parameters indicates that the molecule is weakly absorbed [41]. Genistein has the highest percentage compared to the other third ligands; this can result in a lighter molecular weight than the other third ligands, so this ligand is absorbed more quickly into the body. Skin permeability, or drug delivery through the skin, can be said to have low permeability if it has a log Kp value > -2.5 [41]; the four ligands have values that are close to each other, which indicates that the four ligands are not suitable if the drug is applied intravenously topical. BBB (Blood-Brain Barrier) is a parameter of a drug's ability to cross the brain. If the logBB value is > 0.3 , it can be stated that the ligand quickly passes through the blood-brain barrier, but if it is < -1 , then the ligand is not well distributed to the brain [41].

Among the four ligands, only genistein has a value exceeding -1 , indicating its relatively good distribution in the brain. According to Dwininda *et al.* [42], three substrates—CYP2C29, CYP2C19, and CYP2D6—play crucial roles in drug metabolism within the body. Notably, only genistein is capable of inhibiting the CYP2C29 and CYP2C19 substrates.

Total clearance refers to the amalgamation of hepatic clearance (metabolism in the liver and biliary clearance) and renal clearance (excretion via the kidneys), which is relevant to a drug's bioavailability and aids in determining the dosage required to attain steady-state concentrations [41]. A higher total clearance indicates easier excretion of the compound. Only dicafeoylquinic acid has a value of < 0 , while the other three ligands have a value of > 0 , and the vincosamide ligand is the ligand that has the highest excretion value. The LD_{50} toxicity parameter is classified according to the Globally

Harmonized System (GHS) and is divided into toxicity classes I to VI, with lower classes indicating higher toxicity. Only eriodictyol 7-O-sophoroside falls into class IV, within which the ligand exhibits cytotoxic activity [43]. Regarding skin sensitization parameters, none of the four ligands show sensitivity to the skin, making topical application of the drug safe.

Lipinski's The Rule of Five aims to determine whether drug candidate compounds can penetrate biological membranes and have good permeability. Among the four ligands, only vincosamide and genistein comply with Lipinski's Rule of Five. However, Lipinski's rule is merely an initial screening tool designed to identify compounds with potential for good oral permeability and bioavailability. It is noteworthy that several compounds, including some antibiotics, antifungals, and vitamins, do not adhere to Lipinski's rule [44].

PASS prediction, also known as Prediction of Activity Spectra for Substances, is used to identify novel targets or mechanisms for specific ligands, and vice versa, to uncover new ligands for specific biological targets [45]. A compound's bioactivity is assessed by evaluating its probability of being active (Pa). This probability estimate indicates the likelihood that the compound belongs to a subgroup of active compounds based on molecular structural similarity, commonly found in the "active" subset within the PASS training dataset. The results of the bioactivity prediction show that the four compounds, except vincosamide, have bioactivity as melanin inhibitors with the highest value of 0.731 by eriodictyol 7-O-sophoroside.

Phenolics, alkaloids, and flavonoids—specifically dicafeoylquinic acid, vincosamide, genistein, and eriodictyol 7-O-sophoroside—demonstrated a strong affinity for the receptor protein. This supports the historical use of compounds from these chemical classes as active ingredients in drugs and cosmetics for centuries, particularly as antimelanogenic agents like whitening agents. The results of *in-silico* studies suggest that the potential of *A. platyphyllum* as an antimelanogenic agent is not limited to direct tyrosinase inhibition. Instead, melanogenesis inhibition can occur through more potent pathways, such as the cGMP and PKC- β pathways, as evidenced by the lower binding energy on these proteins compared to tyrosinase.

4. Conclusion

Extracts of *A. platyphyllum* from various solvents have proven to have the potential as antimelanogenic agents through the inhibition of tyrosinase enzyme. Among the three extraction solvents, ethanol extract exhibited the highest tyrosinase inhibition capacity. These studies indicate that the potential of *A. platyphyllum* as an antimelanogenic is not limited to direct tyrosinase inhibition. Melanogenesis inhibition can occur through more potent pathways, such as the cGMP and PKC- β pathways, as evidenced by lower binding energy on these proteins than tyrosinase.

Acknowledgment

The author expresses appreciation to Mr. Taopik Ridwan, SP, the technical manager at the Biopharmaca Conservation and Cultivation Station, Tropical Biopharmaca Research Center, IPB University, for his support in providing samples of *A. platyphyllum*. The author also expresses appreciation to Dr. Setyanto Tri Wahyudi

References

- [1] W. Westerhof, T. J. Kooyers, Hydroquinone and its analogues in dermatology – a potential health risk, *Journal of Cosmetic Dermatology*, 4, 2, (2005), 55–59 <https://doi.org/10.1111/j.1473-2165.2005.40202.x>
- [2] Irmanida Batubara, Rika Indri Astuti, Muhammad Eka Prastya, Auliya Ilmiawati, Miwa Maeda, Mayu Suzuki, Akie Hamamoto, Hiroshi Takemori, The Antiaging Effect of Active Fractions and Ent-11 α -Hydroxy-15-Oxo-Kaur-16-En-19-Oic Acid Isolated from *Adenostemma lavenia* (L.) O. Kuntze at the Cellular Level, *Antioxidants*, 9, 8, (2020), 719 <https://doi.org/10.3390/antiox9080719>
- [3] Eka Budiarti, Irmanida Batubara, Auliya Ilmiawati, Potensi Beberapa Ekstrak Tumbuhan Asteraceae sebagai Antioksidan dan Antiglukasi, *Jurnal Jamu Indonesia*, 4, 3, (2019), 103–111 <https://doi.org/10.29244/jji.v4i3.161>
- [4] Akie Hamamoto, Ryosuke Isogai, Miwa Maeda, Masumi Hayazaki, Eito Horiyama, Shigeo Takashima, Mamoru Koketsu, Hiroshi Takemori, The High Content of Ent-11 α -hydroxy-15-oxo-kaur-16-en-19-oic Acid in *Adenostemma lavenia* (L.) O. Kuntze Leaf Extract: With Preliminary in Vivo Assays, *Foods*, 9, 1, (2020), 73 <https://doi.org/10.3390/foods9010073>
- [5] Lucía de la Torre, Hugo Navarrete, Priscilla Muriel M., Manuel Juan Macía Barco, Henrik Balslev, Enciclopedia de las plantas útiles del Ecuador, *Herbario QCA de la Escuela de Ciencias Biológicas de la Pontificia Universidad Católica del Ecuador*, (2008),
- [6] Nurlela Nurlela, Rifan Nurfalah, Fira Ananda, Taopik Ridwan, Auliya Ilmiawati, Waras Nurcholis, Hiroshi Takemori, Irmanida Batubara, Variation of morphological characteristics, total phenolic, and total flavonoid in *Adenostemma lavenia*, *A. madurense*, and *A. platyphyllum*, *Biodiversitas Journal of Biological Diversity*, 23, 8, (2022), 3999–4005 <https://doi.org/10.13057/biodiv/d230818>
- [7] Mokdad-Bzeouich Imen, Fadwa Chaabane, Mustapha Nadia, Kilani-jaziri Soumaya, Ghedira Kamel, Chekir-Ghedira Leila, Anti-melanogenesis and antigenotoxic activities of eriodictyol in murine melanoma (B16-F10) and primary human keratinocyte cells, *Life Sciences*, 135, (2015), 173–178 <https://doi.org/10.1016/j.lfs.2015.06.022>
- [8] Nadia Tabassum, Ji-Hyung Lee, Soon-Ho Yim, Galzad Javzan Batkhuu, Da-Woon Jung, Darren R. Williams, Isolation of 4,5-O-Dicaffeoylquinic Acid as a Pigmentation Inhibitor Occurring in *Artemisia capillaris* Thunberg and Its Validation In Vivo, *Evidence-Based Complementary and Alternative Medicine*, 2016, (2016), 7823541 <https://doi.org/10.1155/2016/7823541>
- [9] Nurlela Nurlela, Setyanto Tri Wahyudi, Auliya Ilmiawati, Waras Nurcholis, Hiroshi Takemori, Irmanida Batubara, Chemical profiling and computational identification of potential antibacterials from *Adenostemma* species, *South African Journal of Botany*, 162, (2023), 847–863 <https://doi.org/10.1016/j.sajb.2023.10.010>
- [10] Dipak Raj Pant, Narayan Dutt Pant, Uday Narayan Yadav, Dharma Prasad Khanal, Phytochemical screening and study of antioxidant, antimicrobial, antidiabetic, anti-inflammatory and analgesic activities of extracts from stem wood of *Pterocarpus marsupium* Roxburgh, *Journal of Intercultural Ethnopharmacology*, 6, 2, (2017), 170–176 <https://doi.org/10.5455/jice.20170403094055>
- [11] Irmanida Batubara, Iren Julita, Latifah K. Darusman, Ali Mahmoud Muddathir, Tohru Mitsunaga, Flower Bracts of Temulawak (*Curcuma xanthorrhiza*) for Skin Care: Anti-acne and Whitening Agents, *Procedia Chemistry*, 14, (2015), 216–224 <https://doi.org/10.1016/j.proche.2015.03.031>
- [12] Eka Budiarti, Perlambang Budiarti, Manggar Arum Aristri, Irmanida Batubara, Kolagen dari Limbah Tulang Ayam (*Gallus gallus domesticus*) terhadap Aktivitas Anti Aging secara In Vitro, *ALCHEMY Jurnal Penelitian Kimia*, 15, 1, (2019), 44–56 <https://doi.org/10.20961/alchemy.15.1.23046.44-56>
- [13] L. Schrödinger, W. DeLano, in, 2020, <http://www.pymol.org/pymol>
- [14] Yazan Haddad, Vojtech Adam, Zbynek Heger, Ten quick tips for homology modeling of high-resolution protein 3D structures, *PLoS Computational Biology*, 16, 4, (2020), e1007449 <https://doi.org/10.1371/journal.pcbi.1007449>
- [15] Garrett M. Morris, Ruth Huey, William Lindstrom, Michel F. Sanner, Richard K. Belew, David S. Goodsell, Arthur J. Olson, AutoDock4 and AutoDockTools4: Automated docking with selective receptor flexibility, *Journal of Computational Chemistry*, 30, 16, (2009), 2785–2791 <https://doi.org/10.1002/jcc.21256>
- [16] Sunghwan Kim, Jie Chen, Tiejun Cheng, Asta Gindulyte, Jia He, Siqian He, Qingliang Li, Benjamin A. Shoemaker, Paul A. Thiessen, Bo Yu, Leonid Zaslavsky, Jian Zhang, Evan E. Bolton, PubChem 2023 update, *Nucleic Acids Research*, 51, D1, (2022), D1373–D1380 <https://doi.org/10.1093/nar/gkac956>
- [17] Noel M. O'Boyle, Michael Banck, Craig A. James, Chris Morley, Tim Vandermeersch, Geoffrey R. Hutchison, Open Babel: An open chemical toolbox, *Journal of Cheminformatics*, 3, (2011), 33 <https://doi.org/10.1186/1758-2946-3-33>
- [18] Jerome Eberhardt, Diogo Santos-Martins, Andreas F. Tillack, Stefano Forli, AutoDock Vina 1.2.0: New Docking Methods, Expanded Force Field, and Python Bindings, *Journal of Chemical Information and Modeling*, 61, 8, (2021), 3891–3898 <https://doi.org/10.1021/acs.jcim.1c00203>
- [19] Oleg Trott, Arthur J. Olson, AutoDock Vina: Improving the speed and accuracy of docking with a new scoring function, efficient optimization, and multithreading, *Journal of Computational Chemistry*, 31, 2, (2010), 455–461 <https://doi.org/10.1002/jcc.21334>
- [20] Roman A. Laskowski, Mark B. Swindells, LigPlot+: Multiple Ligand-Protein Interaction Diagrams for Drug Discovery, *Journal of Chemical Information and*

- Modeling*, 51, 10, (2011), 2778-2786
<https://doi.org/10.1021/ci200227u>
- [21] Soon Huat Tiong, Chung Yeng Looi, Hazrina Hazni, Aditya Arya, Mohammadjavad Paydar, Won Fen Wong, Shiau-Chuen Cheah, Mohd Rais Mustafa, Khalijah Awang, Antidiabetic and Antioxidant Properties of Alkaloids from *Catharanthus roseus* (L.) G. Don, *Molecules*, 18, 8, (2013), 9770-9784
<https://doi.org/10.3390/molecules18089770>
- [22] Azizah Ugusman, Zaiton Zakaria, Chua Kien Hui, Nor Anita Megat Mohd Nordin, Zaleha Abdullah Mahdy, Flavonoids of *Piper sarmentosum* and its cytoprotective effects against oxidative stress, *EXCLI Journal*, 11, (2012), 705-714
- [23] Fitria Wijayanti, Mayang Sari, Roni Suprayitno, Dian Aminin, The Gel Soap with Raw Materials of Lerak Fruit (*Sapindus rarak* DC), *Stannum: Jurnal Sains dan Terapan Kimia*, 2, 1, (2020), 1-6
<https://doi.org/10.33019/jstk.v2i1.1618>
- [24] Makoto Kondo, Yoshiaki Hirano, Noriyuki Ikai, Kazumi Kita, Anuraga Jayanegara, Hiro-omi Yokota, Assessment of Anti-nutritive Activity of Tannins in Tea By-products Based on *In vitro* Rumen Fermentation, *Asian-Australasian Journal of Animal Sciences*, 27, 11, (2014), 1571-1576
<https://doi.org/10.5713/ajas.2014.14204>
- [25] Fitria Wulandari, Fauzia Ningrum Syaputri, Nanda Raudhatil Jannah, The Effect of Various Concentrations of the Addition of Emulsifier Tween 80 and Span 80 on the Stability of Cream Formulation Ethanolic Extract of Basil Leaves (*Ocimum Americanum* L), *Lambung Farmasi: Jurnal Ilmu Kefarmasian*, 3, 2, (2022), 197-203
- [26] Roxana Ghiulai, Oana Janina Roşca, Diana Simona Antal, Marius Mioc, Alexandra Mioc, Roxana Racoviceanu, Ioana Macaşoi, Tudor Olariu, Cristina Dehelean, Octavian Marius Creţu, Mirela Voicu, Codruţa Şoica, Tetracyclic and Pentacyclic Triterpenes with High Therapeutic Efficiency in Wound Healing Approaches, *Molecules*, 25, 23, (2020), 5557
<https://doi.org/10.3390/molecules25235557>
- [27] A. Fauzan, D. Praseptiangga, R. Hartanto, B. Pujiasmanto, Characterization of the chemical composition of *Adenostemma lavenia* (L.) Kuntze and *Adenostemma platyphyllum* Cass, *IOP Conference Series: Earth and Environmental Science*, 102, (2018), 012029
<https://doi.org/10.1088/1755-1315/102/1/012029>
- [28] The Association of Official Analytical Chemist, *Official Methods of Analysis of AOAC International*, 19th ed., Association of Official Analytical Chemist Inc., Virginia, USA, 2016,
- [29] Fira Ananda, Pertumbuhan, Produksi Fenolik dan Flavonoid *Adenostemma platyphyllum* pada Dosis Pupuk Kandang Sapi yang Berbeda, Chemistry Department, IPB University, 2022
- [30] Gederts Ievinsh, Water Content of Plant Tissues: So Simple That Almost Forgotten?, *Plants*, 12, 6, (2023), 1238
<https://doi.org/10.3390/plants12061238>
- [31] Samaneh Zolghadri, Asieh Bahrami, Mahmud Tareq Hassan Khan, J. Munoz-Munoz, F. Garcia-Molina, F. Garcia-Canovas, Ali Akbar Saboury, A comprehensive review on tyrosinase inhibitors, *Journal of Enzyme Inhibition and Medicinal Chemistry*, 34, 1, (2019), 279-309
<https://doi.org/10.1080/14756366.2018.1545767>
- [32] L. Saghaie, M. Pourfarzam, A. Fassihi, B. %J Research in pharmaceutical sciences Sartippour, Synthesis and tyrosinase inhibitory properties of some novel derivatives of kojic acid, *Research in Pharmaceutical Sciences*, 8, 4, (2013), 233-242
- [33] Satoshi Aida, Yukiko Sonobe, Munehiro Yuhki, Kiyooki Sakata, Toshihiko Fujii, Hiroshi Sakamoto, Takakazu Mizuno, MITF suppression by CH5552074 inhibits cell growth in melanoma cells, *Cancer Chemotherapy and Pharmacology*, 79, 6, (2017), 1187-1193
<https://doi.org/10.1007/s00280-017-3317-6>
- [34] Ya Zhang, Xin Wang, Targeting the Wnt/ β -catenin signaling pathway in cancer, *Journal of Hematology & Oncology*, 13, (2020), 165
<https://doi.org/10.1186/s13045-020-00990-3>
- [35] Arwansyah Arwansyah, Laksmi Ambarsari, Tony I. Sumaryada, Simulasi *docking* senyawa kurkumin dan analognya sebagai inhibitor reseptor androgen pada kanker prostat, *Current Biochemistry*, 1, 1, (2014), 11-19
- [36] Neil Grodsky, Ying Li, Djamel Bouzida, Robert Love, Jordan Jensen, Beverly Nodes, Jim Nonomiya, Stephan Grant, Structure of the Catalytic Domain of Human Protein Kinase C β II Complexed with a Bisindolylmaleimide Inhibitor, *Biochemistry*, 45, 47, (2006), 13970-13981
<https://doi.org/10.1021/bi061128h>
- [37] Xuelei Lai, Harry J. Wichers, Montserrat Soler-Lopez, Bauke W. Dijkstra, Structure of Human Tyrosinase Related Protein 1 Reveals a Binuclear Zinc Active Site Important for Melanogenesis, *Angewandte Chemie International Edition*, 56, 33, (2017), 9812-9815
<https://doi.org/10.1002/anie.201704616>
- [38] Christian Ebere Enyoh, Qingyue Wang, Sex toys for pleasure, but there are risks: *In silico* toxicity studies of leached Micro/Nanoplastics and phthalates, *Hygiene and Environmental Health Advances*, 10, (2024), 100092
<https://doi.org/10.1016/j.heha.2024.100092>
- [39] György G. Ferenczy, Miklós Kellermayer, Contribution of hydrophobic interactions to protein mechanical stability, *Computational and Structural Biotechnology Journal*, 20, (2022), 1946-1956
<https://doi.org/10.1016/j.csbj.2022.04.025>
- [40] S. Grogan, C. V. Preuss, Pharmacokinetics, in: *StatPearls*, StatPearls Publishing
- Copyright © 2024, StatPearls Publishing LLC., Treasure Island (FL) ineligible companies. Disclosure: Charles Preuss declares no relevant financial relationships with ineligible companies., 2024,
- [41] Douglas E. V. Pires, Tom L. Blundell, David B. Ascher, pkCSM: Predicting Small-Molecule Pharmacokinetic and Toxicity Properties Using Graph-Based Signatures, *Journal of Medicinal Chemistry*, 58, 9, (2015), 4066-4072
<https://doi.org/10.1021/acs.jmedchem.5b00104>
- [42] Windy Dwininda, Surya Dwira, Rafika Indah Paramita, Analisis Polimorfisme Gen CYP pada Metabolisme Obat Melalui Pendekatan Bioinformatika, *Pratista Patologi*, 8, 1, (2023), 12-12

- [43] Ayu Reskianingsih, Uji Toksisitas Akut Ekstrak Metanol Buah *Phaleria macrocarpa* (Scheff) Boerl Terhadap Larva *Artemia salina* Leach Dengan Metode *Brine Shrimp Lethality Test* (BSLT), Fakultas Kedokteran dan Ilmu Kesehatan, UIN Syarif Hidayatullah, Jakarta, 2014
- [44] B. G. Giménez, M. S. Santos, M. Ferrarini, J. P. S. Fernandes, J. P. S. Fernandes, Evaluation of blockbuster drugs under the Rule-of-five, *Die Pharmazie - An International Journal of Pharmaceutical Sciences*, 65, 2, (2010), 148-152 <https://doi.org/10.1691/ph.2010.9733>
- [45] Alexey Lagunin, Alla Stepanchikova, Dmitrii Filimonov, Vladimir Poroikov, PASS: prediction of activity spectra for biologically active substances, *Bioinformatics*, 16, 8, (2000), 747-748 <https://doi.org/10.1093/bioinformatics/16.8.747>